Large-Eddy Simulation Using Projection onto Local Basis Functions

S.B. Pope

Mechanical and Aerospace Engineering, Cornell University, Ithaca, NY, 14853

Abstract. In the traditional approach to LES for inhomogeneous flows, the resolved fields are obtained by a filtering operation (with filter width Δ). The equations governing the resolved fields are then partial differential equations, which are solved numerically (on a grid of spacing h). For an LES computation of a given magnitude (i.e., given h), there are conflicting considerations in the choice of Δ: to resolve a large range of turbulent motions, Δ should be small; to solve the equations with numerical accuracy, Δ should be large. In the alternative approach advanced here, this conflict is avoided. The resolved fields are defined by projection onto local basis functions, so that the governing equations are ordinary differential equations for the evolution of the basis-function coefficients. There is no issue of numerical spatial discretization errors. A general methodology for modelling the effects of the residual motions is developed. The model is based directly on the basis-function coefficients, and its effect is to smooth the fields where their rates of change are not well resolved by the basis functions. Demonstration calculations are performed for Burgers' equation.

1 Introduction

We reconsider here the fundamentals of large-eddy simulation (LES) for inhomogeneous turbulent flows. The basic idea of LES is to represent explicitly the large-scale turbulent motions, and to model the effects of the small-scale motions (see, e.g., Leonard 1974, Reynolds 1990, Galperin and Orszag 1993, Pope 2000). In the usual approach to LES (see Fig. 1) the steps are as follows:

1. A filtering operation is used to decompose the velocity $\mathbf{U}(\mathbf{x},t)$ into a *resolved field* $\overline{\mathbf{U}}(\mathbf{x},t)$—which represents the large-scale motions—and a *residual field* $\mathbf{u}'(\mathbf{x},t)$—representing the small-scale motions. For the inhomogeneous flows considered, a box filter or a Gaussian filter is the usual choice, or the filter may not be explicitly specified.
2. The conservation equations for $\overline{\mathbf{U}}$ are derived from the Navier-Stokes equations. These contain, as an unknown, the residual-stress tensor τ_{ij}^r, which embodies the effect of the residual motions on the resolved velocity.
3. The equations for $\overline{\mathbf{U}}$ are closed by modelling the residual stresses. Usually the eddy-viscosity Smagorinsky model is used, possibly in conjunction with the dynamic procedure (Germano et al. 1991), and in combination with other models.

J.L. Lumley (Ed.): LNP 566, pp. 239–265, 2001.

4. In order to solve the partial differential equations (PDE's) governing $\overline{\mathbf{U}}(\mathbf{x}, t)$, a grid is generated to discretize the flow domain. The filter width Δ is taken to be proportional to the local grid spacing h.
5. The PDE's for $\overline{\mathbf{U}}(\mathbf{x}, t)$ are solved numerically.
6. The accuracy of the overall procedure can be assessed by comparing statistics of the calculated resolved fields to those obtained from the Navier-Stokes equations (by experiment or by DNS).

In the following two subsections we raise two issues with this standard approach. The remainder of the paper addresses a resolution to the second of these issues.

1.1 Quantification and Control of the Scale of the Resolved Motions

An important issue is the size range of the turbulent motions resolved, which is determined by the size of the filter width Δ relative to the turbulence integral scale L (or to the viscous lengthscale in the viscous near-wall region). How much of the turbulent motions are resolved can be quantified by the fraction of the turbulence energy contained in the resolved scales. Pope (2000) suggests a distinction between LES and VLES (very large-eddy simulation) depending upon whether more or less than 80% of the turbulence energy is resolved. (In the viscous near-wall region, unless wall-function boundary conditions are used, LES then requires that the filter width be comparable to the viscous lengthscale—though substantially larger than DNS grid spacings.)

The general experience is that LES (with at least 80% of the energy resolved) produces good results in free shear flows, and also for simple wall-bounded flows if the dynamic model is used (see, e.g., Vreman et al. 1997, Piomelli 1993). In contrast, the results with VLES can be unpredictable and poor (see, e.g., Rodi et al. 1997).

In order for LES to be a robust and reliable tool, it is necessary to require that the fraction of turbulence energy resolved be greater than some minimum—say 80%. This requires: (a) a methodology to estimate (locally within the LES) the fraction of energy resolved; and (b) a methodology to adapt the filter width Δ (and hence the grid spacing h) to ensure that 80% of the energy is resolved.

Note that in the standard approach the grid—and hence the filter width—are specified *a priori*, and hence either prior knowledge of the flow is required, or 80% resolution is not assured.

1.2 Numerical Resolution of Resolved Fields

The filtering operation (using the box or Gaussian filters) produces infinite-dimensional resolved fields $\overline{\mathbf{U}}(\mathbf{x}, t)$. These fields have to be discretized in order to solve their governing PDE's computationally. This involves a discretization

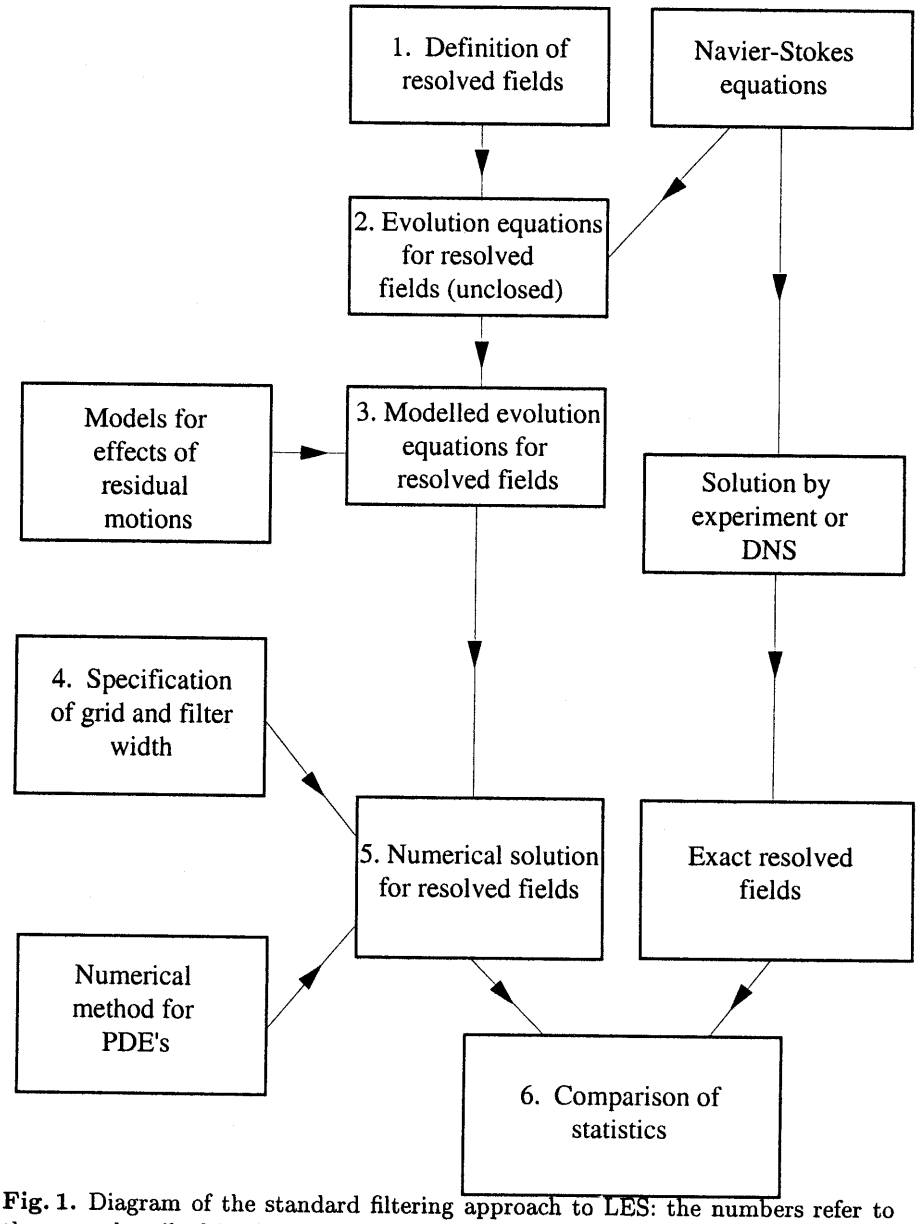

Fig. 1. Diagram of the standard filtering approach to LES: the numbers refer to the steps described in the Introduction.

error that depends on the grid size h relative to the filter width Δ. For the inhomogeneous flows that arise in engineering applications, most suited are unstructured-grid methods which are generally (at most) second-order accurate, so that the discretization error scales as $(h/\Delta)^2$ (when this ratio is small). Good numerical resolution comes at a high cost: halving h decreases the numerical error by a factor of 4, but it increases the memory requirements by a factor of 8, and the number of operations by a factor of 16.

Note that the word "resolution" is used here in two different senses. The range of turbulent scales resolved by the (exact) filtered fields $\overline{\mathbf{U}}(\mathbf{x},t)$ is determined by the ratio Δ/L (away from walls). The accuracy of the numerical resolution of $\overline{\mathbf{U}}(\mathbf{x},t)$ on a grid of spacing h is determined by the ratio h/Δ.

There is a trade-off between resolution of the turbulent motions and numerical resolution. For an LES (or VLES) performed on a given grid of spacing h, consider the two choices of filter width: $\Delta = 2h$ and $\Delta = h$. The former yields moderately good numerical resolution. The latter yields poor numerical resolution, but the range of turbulent motions resolved is doubled. In engineering applications the latter choice is usual, so that numerical errors can be substantial.

This trade-off between resolution of the turbulent motions and numerical resolution can be completely avoided by *defining* the resolved fields to be finite-dimensional. This can be achieved through a basis-function representation of the form

$$\overline{\mathbf{U}}(\mathbf{x},t) = \sum_{\alpha=1}^{N} \hat{u}_\alpha(t)\mathbf{b}_\alpha(\mathbf{x}), \tag{1}$$

where $\mathbf{b}_\alpha$, $\alpha = 1,2,...,N$ is a set of vector-valued basis functions, and $\hat{u}_\alpha(t)$ are the corresponding basis-function coefficients. (Alternatively the basis functions can be scalar-valued and the coefficients vector-valued.) Given a velocity field $\mathbf{U}(\mathbf{x},t)$, the corresponding resolved field is defined as a projection of $\mathbf{U}$ onto the basis functions. Here, for simplicity, we consider the orthogonal projection, so that the basis-function coefficients are determined by the equivalent condition that the kinetic energy of the residual motions

$$\int \tfrac{1}{2}(\mathbf{U}-\overline{\mathbf{U}})\cdot(\mathbf{U}-\overline{\mathbf{U}})\,\mathrm{d}\mathbf{x} \tag{2}$$

be minimized (where integration is over the flow domain).

In this approach, evolution equations for the resolved fields take the form of a set of ordinary differential equations (ODE's) for the basis-function coefficients: there is no issue of the numerical spatial resolution of the resolved fields.

The idea of using a finite basis-function representation of the resolved fields is far from new. It is done in LES of homogeneous turbulence using the sharp spectral filter, in which case the basis functions are Fourier modes. And it is done in dynamical system models of inhomogeneous flows, in which

case the basis functions are taken to be the POD eigenfunctions (see, e.g., Holmes et al. 1996). In both of these cases the basis functions are orthogonal and global—that is, the basis functions are non-zero everywhere in the flow domain (except on a set of measure zero). In contrast, here, for application of LES to complex flows, we have in mind non-orthogonal local basis functions (which are zero over most of the domain). Examples of such basis functions are B-splines and finite-elements. Accordingly, the method advanced here can be called large-eddy simulation using projection onto local basis functions, or LES-PLB for short. The different approaches mentioned are summarized in Table 1. As indicated in the table, the basis functions considered here are non-orthogonal.

If an LES is performed with N grid nodes or N basis functions, then an important consideration is the scaling with N of the number of operations required to evaluate the non-linear convective terms in the momentum equations. In the direct implementation of basis-function or spectral methods, of order N^2 operations are required, because the non-linear convective term appears as double-sum over the N basis-function coefficients. This number of operations can be reduced, however, if the basis functions have a special structure. If a first transform exists, then a pseudo-spectral method can be used, reducing the number of operations to of order N log N. Or if (as is the case with LES-PLB) at every point in the domain the number of non-zero basis functions is less than a fixed number (independent of N), then there are only of order N non-zero contributions to the double sum. These considerations are summarized in the last column of Table 1.

As mentioned above, the types of basis functions suitable for LES-PLB include finite-elements and B-splines, and the formulation developed below is closely connected to the Galerkin method. Both finite elements and B-splines have been used previously in LES (see, e.g., Haworth & Jansen 2000, Kravchenko et al. 1996). It should be appreciated, however, that the present approach is fundamentally different. Here we *define* the resolved fields by a basis-function representation, so that the governing equations are ODE's. In contrast, in previous work finite elements and B-splines, have been used to obtain numerical solutions to the PDEs governing the filtered fields. The semi-discrete equations arising from these approaches are also ODEs for basis function coefficients; but it should be appreciated that an approximation is involved in obtaining these ODEs from the PDEs. There is no such approximation in LES-PLB.

1.3 Outline of the Paper

In the remainder of the paper the LES-PLB methodology is developed and demonstrated. In Section 2 the general formulation is given. It is shown that if the turbulent motions are fully resolved (i.e., DNS rather than LES), then the result is the Galerkin method to solve the governing equations. In Section 3 a model for the effects of the residual motions is proposed.

Table 1. Comparison of approaches to large-eddy simulation.

	Governing equations	Support of basis functions	Orthogonality	Number of operations for convective terms
LES with filtering in physical space	PDE's	—	—	N
LES with sharp spectral filter	ODE's	global	orthogonal	$N\log(N)$
LES using POD eigenfunctions	ODE's	global	orthogonal	N^2
LES-PLB	ODE's	local	non-orthogonal	N

While the ultimate intended application is to complex flows governed by the Navier-Stokes equations, the method is demonstrated in the simpler setting of Burgers' equation (Burgers 1940). The scalar velocity $u(x,t)$ evolves by

$$\frac{\partial u}{\partial t} + u\frac{\partial u}{\partial x} = \nu\frac{\partial^2 u}{\partial x^2} + f, \tag{3}$$

where ν is the viscosity and $f(x,t)$ is the forcing. Previous studies of Burgers' equation include: Saffman (1967), Gotoh and Kraichnan (1993) and Girimaji and Zhou (1995). In Section 4 the LES-PLB method is applied to Burgers' equation using linear-spline basis functions.

Even though the demonstration given here uses simple 1D basis functions and Burgers' equation, it is stressed that the methodology is general, and intended for complex 3D flows governed by the Navier-Stokes equations.

2 Formulation of LES using Local Basis Functions

For simplicity we consider a one-dimensional formulation of Burgers' equation, but all of the concepts and results have straightforward extensions to the Navier-Stokes equations in 3D. The domain is of length $\mathcal{L}$, and periodic boundary conditions are applied, i.e., $u(x,t) = u(x + k\mathcal{L}, t)$, for all integer k.

We introduce a set of N basis functions, $b_j(x)$, $j = 1, 2, ..., N$. Later we consider linear and parabolic spline basis functions, with uniform knot spacing $h = \mathcal{L}/N$. But for the present, we make no particular specification of $b_j(x)$.

Given a function $u(x)$, the corresponding resolved field $\overline{u}(x)$ is defined as the orthogonal projection of $u(x)$ onto the basis functions:

$$\overline{u}(x) \equiv \mathcal{P}\{u(x)\} = \sum_{j=1}^{N} b_j(x)\hat{u}_j, \tag{4}$$

where $\mathcal{P}$ is the projection operator, and the basis-function coefficients $\hat{u}_j$ are determined by the condition that they minimize

$$\chi \equiv \frac{1}{\mathcal{L}} \int_0^{\mathcal{L}} [\overline{u}(x) - u(x)]^2 \, \mathrm{d}x. \tag{5}$$

It is readily shown that the basis-function coefficients are given explicitly by

$$\hat{u}_j = \mathcal{P}_j\{u(x)\} \equiv M_{jk}^{-1} Q_k\{u(x)\}, \tag{6}$$

where the operator $Q_k\{\ \}$ is defined by

$$Q_k\{u(x)\} \equiv \int_0^{\mathcal{L}} b_k(x)u(x) \, \mathrm{d}x, \tag{7}$$

M_{jk}^{-1} is the j-k component of the inverse of the positive symmetric definite matrix

$$M_{jk} \equiv \int_0^{\mathcal{L}} b_j(x)b_k(x) \, \mathrm{d}x, \tag{8}$$

and summation is implied over repeated suffixes.

From Eqs. (4) and (7) it is straightforward to show that $\mathcal{P}\{\ \}$ is indeed a projection, i.e.,

$$\mathcal{P}\{\overline{u}(x)\} = \mathcal{P}\{\mathcal{P}\{u(x)\}\} = \overline{u}(x), \tag{9}$$

and equivalently

$$\mathcal{P}\{u'(x)\} = 0, \tag{10}$$

for the residual

$$u'(x) \equiv u(x) - \overline{u}(x). \tag{11}$$

We consider the general evolution equation for $u(x,t)$

$$\frac{\partial u}{\partial t} = A(u), \tag{12}$$

where, for Burgers' equation (Eq. 3), the functional $A(u)$ is defined by

$$A(u) \equiv -u\frac{\partial u}{\partial x} + \nu\frac{\partial^2 u}{\partial x^2} + f. \tag{13}$$

Since the basis functions are independent of time, the corresponding evolution equation for $\overline{u}(x,t)$ is

$$\frac{\partial \overline{u}}{\partial t} = \frac{\partial}{\partial t}\mathcal{P}\{u\} = \mathcal{P}\{\frac{\partial u}{\partial t}\} = \mathcal{P}\{A(u)\}, \tag{14}$$

or, for the basis-function coefficients,

$$\frac{\mathrm{d}\hat{u}_j}{\mathrm{d}t} = \mathcal{P}_j\{A(u)\} = \mathcal{P}_j\{A(\overline{u} + u')\}, \tag{15}$$

where the operator $\mathcal{P}_j$ is defined by Eq. (6). In LES, $\overline{u}$ is known whereas u' is unknown, so that the right-hand side of Eq. (15) is unknown. The equation can be rewritten

$$\frac{\mathrm{d}\hat{u}_j}{\mathrm{d}t} = \mathcal{P}_j\{A(\overline{u})\} + R_j, \tag{16}$$

where the term

$$R_j \equiv \mathcal{P}_j\{A(u)\} - \mathcal{P}_j\{A(\overline{u})\}, \tag{17}$$

embodies the effects of the residual motions that have to be modelled. Thus, the two terms on the right-hand side of Eq. (16) are, respectively, the known contribution from the resolved field, and the contribution from the residual field that has to be modelled. The modelling of R_j is the subject of the next section.

An interesting limit to consider is that in which the basis functions are sufficient to resolve $u(x)$ accurately, so that u' and R_j are negligible. This circumstance corresponds to DNS rather than LES, and Eq. (16) reduces to

$$\frac{\mathrm{d}\hat{u}_j}{\mathrm{d}t} = \mathcal{P}_j\{A(\overline{u})\}. \tag{18}$$

This is simply a statement of the Galerkin method to solve Eq. (12). The details are given in Appendix A for Burgers' equation using linear splines. It is again emphasized, however, that LES-PLB is distinctly different from using a Galerkin method to solve the filtered equations.

3 Modelling the Effects of the Residual Motions

3.1 Guiding Principles

The residual motions $u'(x,t)$ affect the resolved motions through the quantity R_j defined by Eq. (17). We propose a model for R_j which is based on three tenets:

1. The model is based directly on basis-function coefficients.
2. The magnitude of the modelled term is significant only in regions where $A(\overline{u})$ is not well resolved by the basis functions.
3. The effect of the modelled term is to increase the smoothness of the resolved field $\overline{u}$.

In opposition to tenet (1) we could consider a standard eddy-viscosity model of the form

$$\frac{\partial \overline{u}}{\partial t} = \ldots \frac{\partial}{\partial x}(\nu_r \frac{\partial \overline{u}}{\partial x}), \tag{19}$$

where $\nu_r(x)$ is the residual viscosity, perhaps obtained from the Smagorinsky model. But this term is not exactly representable in terms of the basis functions, and so it has to be implemented via a numerical method that inevitably incurs a spatial discretization error. This clearly runs counter to the philosophy of the present approach in that numerical resolution becomes an issue. In view of these considerations, we perform the modelling on R_j in terms of $\hat{u}_k$ (i.e., in terms of basis-function coefficients rather than fields) so that there are no numerical resolution issues.

Tenets (2) and (3) are similar to those of the MILES approach (monotone integrated large-eddy simulations) as articulated by Boris et al. (1992). In simple methods for the numerical solution of PDE's—e.g., centered finite-difference schemes, pseudo-spectral methods, and the Galerkin method—numerical instabilities arise if the fields are not adequately resolved. The idea of tenet (2) is to make the residual model negligibly small except in regions where, without the modelled term, the solution would become unstable. And the idea of tenet (3) is to impose smoothness directly, thus countering the instability.

Evidently, the modelling approach advocated here is based more on numerical considerations than on the physical consideration used to motivate the dynamic Smagorinsky model, for example. Some justification for the numerical approach is provided by the following observations:

a) for a given number of degrees of freedom (grid nodes or basis functions), the MILES and LES-PLB approaches are able to resolve a greater range of turbulent motions (greater say by a factor of two).

b) it is well appreciated based on *a priori* testing that, at a detailed level, the dynamic Smagorinsky model provides a poor representation of the residual stresses.

3.2 Simple Relaxation Model

The form of the model proposed is

$$R_j = \Omega_{(j)}(\tilde{u}_j - \hat{u}_j), \tag{20}$$

so that the basis-function coefficients evolve by

$$\frac{\mathrm{d}\hat{u}_j}{\mathrm{d}t} = \mathcal{P}_j\{A(\overline{u})\} + \Omega_{(j)}(\tilde{u}_j - \hat{u}_j). \tag{21}$$

(Bracketed suffixes are excluded from the summation convention.) Thus the model causes $\hat{u}_j$ to relax towards the value $\tilde{u}_j$ at the rate $\Omega_{(j)}$: it remains to

specify the two quantities $\tilde{u}_j$ and $\Omega_{(j)}$. (The final model, Eq. 34 below, is a slight modification to the form given here.)

3.3 Relaxation Towards Smooth Fields

The specification of $\tilde{u}_j$ is based on tenet (3). The lack of smoothness in the resolved field is quantified by the pth-order tortuosity, defined by

$$\begin{aligned} T^{(p)} &\equiv \int_0^{\mathcal{L}} \left(\frac{\partial^p \overline{u}}{\partial x^p} \right)^2 \mathrm{d}x \\ &= \hat{u}_j \hat{u}_k M_{jk}^{(p)}, \end{aligned} \tag{22}$$

where the positive definite symmetric matrix $M_{jk}^{(p)}$ is

$$M_{jk}^{(p)} \equiv \int_0^{\mathcal{L}} b_j^{(p)}(x)\, b_k^{(p)}(x)\, \mathrm{d}x, \tag{23}$$

and $b_j^{(p)}(x)$ denotes the pth derivative of the basis function. (For linear splines, only $T^{(1)}$ is defined, because only the first derivatives of $b_j(x)$ are square-integrable. For parabolic splines, both $T^{(1)}$ and $T^{(2)}$ are defined.)

For an appropriately chosen value of p, $\tilde{u}_j$ is defined as the value of $\hat{u}_j$ that minimized $T^{(p)}$, for fixed values of the other basis-function coefficients (i.e., $\hat{u}_k$, $k \neq j$). It is readily shown from Eq. (22) that $\tilde{u}_j$ is given explicitly by

$$\tilde{u}_j = -\sum_{i \neq j} M_{j(i)}^{(p)} \hat{u}_{(i)} / M_{(j)(j)}^{(p)}, \tag{24}$$

and hence the model for R_j (Eq. 20) is

$$R_j = -\Omega_{(j)} \hat{M}_{ji}^{(p)} \hat{u}_i, \tag{25}$$

with

$$\hat{M}_{ji}^{(p)} \equiv M_{ji}^{(p)} / M_{(j)(j)}^{(p)}. \tag{26}$$

Note that the diagonal elements of $\hat{M}_{ji}$ are unity. For linear splines, the non-zero off-diagonal elements of $\hat{M}_{ji}^{(1)}$ are

$$\hat{M}_{(j)(j\pm1)}^{(1)} = -\tfrac{1}{2}. \tag{27}$$

Hence, for this case, the model is

$$\begin{aligned} R_j &= \Omega_{(j)} (\tfrac{1}{2}\hat{u}_{j-1} - \hat{u}_j + \tfrac{1}{2}\hat{u}_{j+1}) \\ &= \tfrac{1}{2}\Omega_{(j)} h^2 \left[\frac{\hat{u}_{j-1} - 2\hat{u}_j + \hat{u}_{j+1}}{h^2} \right], \end{aligned} \tag{28}$$

which evidently is similar to an eddy viscosity model with $\nu_r = \frac{1}{2}\Omega_{(j)}h^2$.

Alternatively, the same analysis for parabolic splines and $p = 2$ leads to the model

$$R_j = -\tfrac{1}{6}h^4\Omega_{(j)}\left[\frac{\hat{u}_{j-2} - 4\hat{u}_{j-1} + 6\hat{u}_j - 4\hat{u}_{j+1} + \hat{u}_{j+2}}{h^4}\right], \tag{29}$$

corresponding to fourth-order dissipation. (Note that the term in square brackets has the form of a finite-difference approximation to a fourth derivative, but $\overline{u}(x)$ is only once continuously differentiable.)

3.4 Relaxation Rate

The specification of $\Omega_{(j)}$ is based on tenet (2): it is significant only where $A(\overline{u})$ is not well resolved by the basis functions.

The quantity a_j, defined by

$$a_{(j)}^2 \equiv \mathcal{P}_j\{[A(\overline{u}) - \mathcal{P}\{A(\overline{u})\}]^2\}, \tag{30}$$

is computable from the resolved field (i.e., from $\{\hat{u}_j\}$) and it measures the extent to which $A(\overline{u})$ is not resolved by the basis functions. Suppose that, in the vicinity of the jth basis function, the velocity $\overline{u}$ is varying very smoothly. Then the residual $A(\overline{u}) - \mathcal{P}\{A(\overline{u})\}$ is small, and so also therefore is $a_{(j)}$. (The right-hand side of Eq. (30) can be evaluated either as a multiple sum over basis function coefficients and integrals of basis function products, or by numerical quadrature: the latter approach is simpler and is used in the calculations presented below.)

From $a_{(j)}$ (which has dimensions of u/t) quantities with the same dimensions as $\Omega_{(j)}$ (i.e., dimensions of $1/t$) can be formed as:

$$\left(\frac{a_{(j)}}{h}\right)^{\frac{1}{2}} \quad \text{or} \quad \frac{a_{(j)}}{v_{(j)}},$$

where $v_{(j)}$ has dimensions of u. It is usual in LES to take the grid spacing h as the relevant lengthscale, which suggests taking $\Omega_{(j)}$ to be proportional to $[a_{(j)}/h]^{\frac{1}{2}}$. We argue, however, that the methodology should be applicable to any field, not just to a velocity field. That is, the modelling should be applicable if u were a temperature field, for example, in which case this specification is dimensionally incorrect. Therefore we take $\Omega_{(j)}$ to be proportional to $a_{(j)}/v_{(j)}$ and define the local scale of u (in this case velocity) by

$$v_{(j)}^2 \equiv \mathcal{R}_j\{[\overline{u}(x) - \mathcal{R}_j\{\overline{u}(x)\}]^2\}, \tag{31}$$

where $\mathcal{R}_j\{\ \}$ is the basis-function average

$$\mathcal{R}_j\{\overline{u}(x)\} \equiv \frac{\int_0^{\mathcal{L}} |b_j(x)|\overline{u}(x)\,\mathrm{d}x}{\int_0^{\mathcal{L}} |b_j(x)|\,\mathrm{d}x}. \tag{32}$$

Then, $\Omega_{(j)}$ is specified as

$$\Omega_{(j)} = \frac{c_r a_{(j)}}{v_{(j)}}, \tag{33}$$

where c_r is a constant to be specified.

3.5 Generalized Relaxation Model

The simple relaxation model described above is modified to ensure the satisfaction of two basic requirements:

1. If the resolved field is uniform (i.e., $\overline{u}(x) = c = \text{constant}$) then the modelled term R_j is identically zero.
2. The effect of the modelled term is to transfer momentum (locally), not to create or destroy momentum.

The momentum conservation principle is well known and readily demonstrated both for the Navier-Stokes and Burgers' equations.

In order to satisfy these requirements, the simple relaxation model (Eq. 20) is generalized to

$$R_j = \omega_{ji}\hat{u}_i, \tag{34}$$

where ω_{ji} is a coefficient matrix to be specified. The simple model developed above corresponds to the specification

$$\omega_{ji} = -\Omega_{(j)}\hat{M}_{ji}^{(p)}. \tag{35}$$

The details of the modification of ω_{ji} given by Eq. (35) to satisfy the above two requirements are given in Appendix B. In the case of 1D linear splines the resulting model is

$$\begin{aligned} R_j = \{ & \tfrac{1}{4}h^2[\Omega_{(j)} + \Omega_{(j+1)}][\hat{u}_{j+1} - \hat{u}_j]/h \\ & - \tfrac{1}{4}h^2[\Omega_{(j)} + \Omega_{(j-1)}][\hat{u}_j - \hat{u}_{j-1}]/h\}/h, \end{aligned} \tag{36}$$

which has the form of a finite-difference approximation to the conservative eddy viscosity term

$$\frac{\partial}{\partial x}\left[\nu_r \frac{\partial \overline{u}}{\partial x}\right], \tag{37}$$

with spatially-varying residual viscosity $\frac{1}{2}\Omega h^2$.

It may be noted that in the (unlikely) case of $\Omega_{(j)}$ being the same for all j, this model (Eq. 36) reverts to the simple model (Eq. 28).

4 Application to the Decay of a Single Mode

In this section and the next, the LES-PLB method described above is applied to two rather different cases of Burgers' equation. Here the Burgers' equation is solved without forcing from a sinusoidal initial condition. In the next section the equation is solved with forcing, which leads to a random, statistically-stationary solution—Burgers' turbulence. The ODE's for the basis function coefficients are integrated in time using a second-order accurate predictor-corrector scheme.

4.1 Description of the Flow

Burgers' equation (Eq. 3) is solved without forcing ($f = 0$) on a periodic domain of length $\mathcal{L} = 2\pi$, from the initial condition

$$u(x, 0) = u_0 \cos(2\pi x/\mathcal{L}), \tag{38}$$

where the velocity scale is $u_0 = 1$. The single non-dimensional parameter in the problem is the Reynolds number

$$\mathrm{Re} \equiv \frac{u_0 \mathcal{L}}{\nu}. \tag{39}$$

Figure 2 shows the evolution of the solution for $\mathrm{Re} = 800$. As may be seen, a "shock" evolves at $x/\mathcal{L} = \frac{1}{4}$. The thickness of the shock scales as $\mathcal{L}\mathrm{Re}^{-1}$, and the peak negative velocity gradient as $\mathrm{Re}\, u_0/\mathcal{L}$.

Figure 3 shows that the evolution of the maximum velocity $u_{max}(t)$ in the domain. It may be seen that u_{max} decreases slowly until the shock develops (at $t \approx 1.5$), and thereafter it decreases more rapidly.

The results shown in Figs. 2 and 3 are obtained by solving the Burgers' equation using the Galerkin method derived in Appendix A. In order to resolve the shock accurately, at least 1,024 linear-spline basis functions are required.

4.2 LES using Projection onto Local Basis Functions

Results are now described of applying the LES-PLB methodology. That is, the coupled set of ODE's (Eq. 16) is solved, in which the effects of the residual motion R_j are modelled by Eq. (36). Only 64 linear-spline basis-function coefficients are used, which clearly is insufficient to resolve the shock.

In Figs. 4 and 5 the LES-PLB solutions are shown for the values of the parameter $c_r = 0$, 0.1, 1.0 and 10, and they are compared to the DNS results.

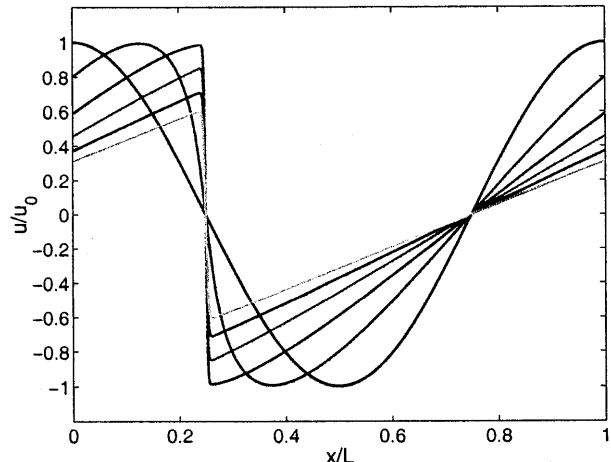

Fig. 2. Solution to Burgers' equation at $tu_0/\mathcal{L} = 0, 1, 2, 3, 4$ from the sinusoidal initial condition and Re = 800. (The value of $u(0,t)$ decreases with time.)

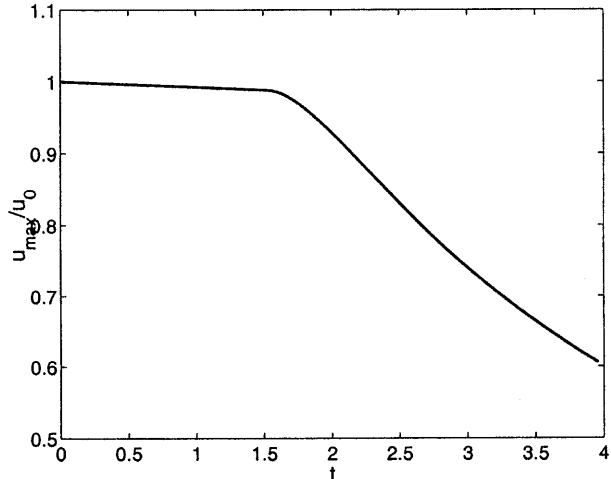

Fig. 3. Evolution of the maximum value of $u(x,t)/u_0$ for the sinusoidal initial condition and Re = 800.

It may be seen from Fig. 4 that the LES-PLB calculations with $c_r = 1.0$ agree well with the DNS, whereas if no model is used (i.e., $c_r = 0$) then u_{max} has a significant overshoot.

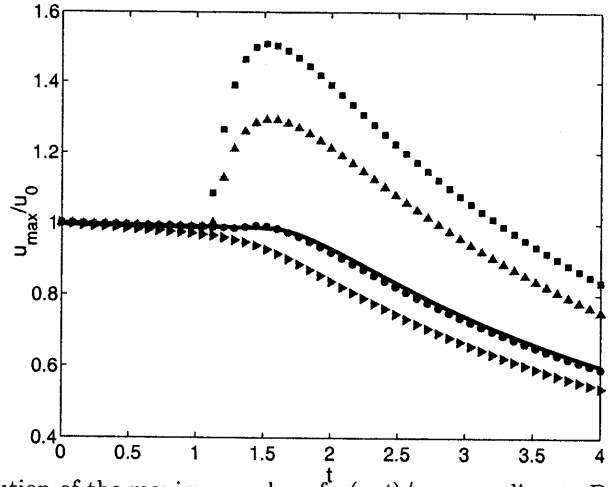

Fig. 4. Evolution of the maximum value of $u(x,t)/u_0$ according to DNS (line) and LES-PLB with $N = 64$ and $c_r = 0$, ■; $c_r = 0.1$, ▲; $c_r = 1.0$, ●; $c_r = 10$, ▶.

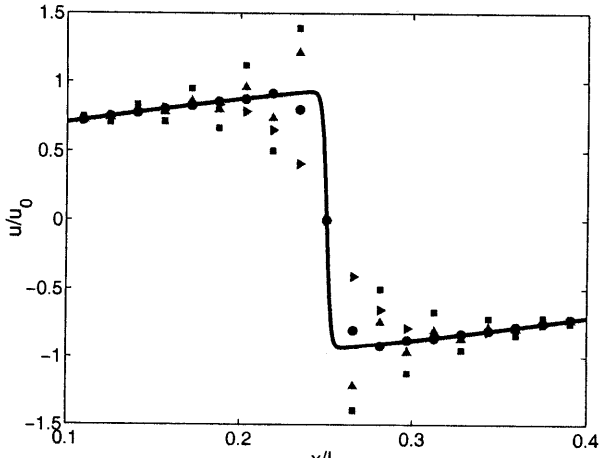

Fig. 5. Profile of $u(x,t)$ through the shock at $t = 2$. Symbols same as Fig. 4.

Figure 5 shows the shock region in more detail at $t = 2$. Evidently, the results with $c_r = 1.0$ are as good as could be expected: the profile is reproduced as accurately as possible with the given number of basis functions.

In contrast, the results with $c_r = 0$ and $c_r = 0.1$ exhibit oscillations and overshoots; whereas with $c_r = 10$ the shock is excessively smeared.

4.3 Comparison with the Smagorinsky Model

The filtered Burgers' equation incorporating the Smagorinsky model is

$$\frac{\partial \overline{u}}{\partial t} + \overline{u}\frac{\partial \overline{u}}{\partial x} = \frac{\partial}{\partial x}\left([\nu + \nu_r]\frac{\partial \overline{u}}{\partial x}\right), \tag{40}$$

where the residual eddy viscosity is

$$\nu_r = \sqrt{2}\ell_s^2\left|\frac{\partial u}{\partial x}\right|, \tag{41}$$

and ℓ_s is the Smagorinsky length-scale, which is specified. It is usual to relate ℓ_s to the filter width Δ via the Smagorinsky constant, i.e.,

$$\ell_s = C_s\Delta, \tag{42}$$

but this is unnecessary.

It is important to appreciate that Eqs. (40) and (41) define a PDE (with ℓ_s as a parameter) independent of a grid. With $\ell_s = 0$, Eq. (40) reverts to Burgers' equation, for which over 1,000 basis functions are required to obtain an accurate solution (using the Galerkin method of Appendix A).

It is found that the specification $\ell_s = 0.06$ (i.e., $\ell_s/\mathcal{L} = 0.03/\pi$) yields solutions similar to those obtained by LES-PLB with 64 basis functions. In Fig. 6, the LES-PLB solution ($N = 64$, $c_r = 1.0$) is compared to the accurate Smagorinsky model ($\ell_s = 0.06$), and indeed there is little difference. Also shown in the figure is the (approximate) Smagorinsky solution obtained on a grid of 64 nodes: the numerical error is evident. To examine this further, Fig. 7 shows the evolution of u_{max} according to the Smagorinsky model calculated on grids of size 64, 128 and 1,024. Even on the 128 grid the numerical errors are evident.

The important point that these results illustrate is that numerical resolution is not an issue in LES-PLB. With conventional LES (using the Smagorinsky model) comparable results are obtained on a finer grid; but there are significant numerical errors if the solution is computed using the same number of basis functions as in LES-PLB. (These errors depend, of course, on the numerical method, and would be expected to be smaller if a higher-order method were used.)

5 Application to Forced Burgers' Turbulence

The LES-PLB methodology is applied here to Burgers' equation with the random forcing using by Gotoh (1999). This results in a statistically-stationary solution.

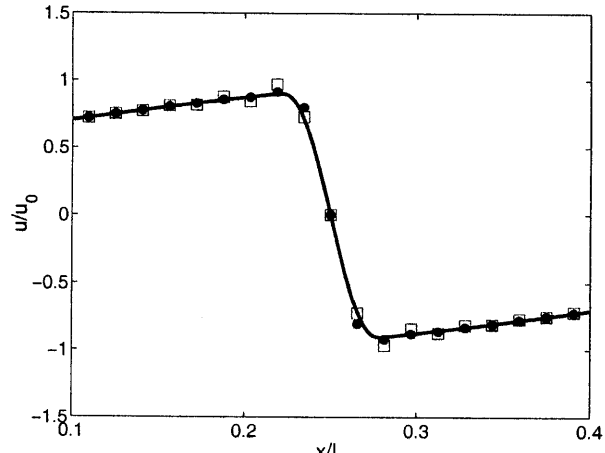

Fig. 6. Profiles of $u(x,t)$ through the shock at $t = 2$. Comparison of LES-PLB ($N = 64$, $c_r = 1.0$, ●) with the Smagorinsky model (accurate calculation, line; using $N = 64$, □).

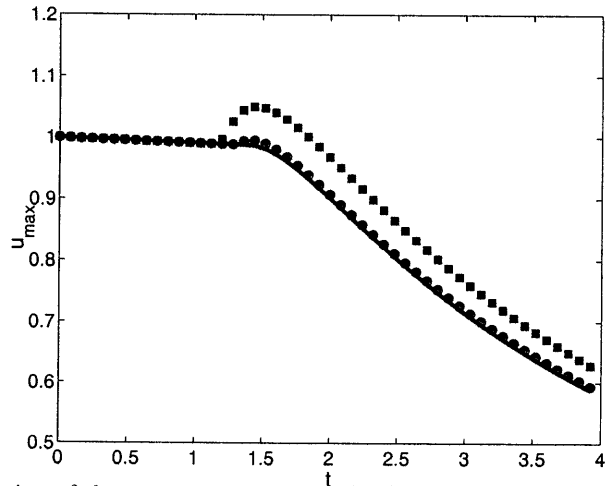

Fig. 7. Evolution of the maximum value of $u(x,t)/u_0$ according to numerical solution of Smagorinsky model: $N = 64$, ■; $N = 128$, ●; $N = 1,024$, line.

The forcing function $f(x,t)$ is white in time and has the wavenumber spectrum

$$\hat{F}(\kappa) = \left(\frac{16}{15\sqrt{\pi}}\right) \frac{\xi_f}{\kappa_f} \left(\frac{\kappa}{\kappa_f}\right)^4 \exp\left(-\left[\frac{\kappa}{\kappa_f}\right]^2\right). \tag{43}$$

This involves two parameters: the forcing wavenumber κ_f, and the forcing magnitude ξ_f (which has dimensions of $\xi \equiv \partial u/\partial x$). The periodic domain is of length $\mathcal{L} = 2\pi$, so that the lowest wavenumber is $\kappa_0 = 1$. The only other parameter in the problem is the viscosity ν. From the four dimensional quantities (κ_0, κ_f, ξ_f and ν) there are two independent non-dimensional groups. We take these to be

$$\frac{\kappa_f}{\kappa_0} = 6, \tag{44}$$

and

$$\mathrm{Re} \equiv \frac{\xi_f}{\nu k_f^2} = 100, \tag{45}$$

to match Gotoh's Run 3.

From the trivial initial condition ($u(x,0) = 0$) Burgers' equation is solved (with or without using LES-PLB) until a statistically-stationary state is reached. The solution is then continued for some time in order to obtain time-averaged statistics.

A sample of $u(x,t)$ in the statistically-stationary state is shown in Fig. 8. It may be seen that there are several "shocks", where the value of u drops abruptly. This is more evident in Fig. 9 which shows the corresponding values of the gradient $\xi \equiv \partial u/\partial x$.

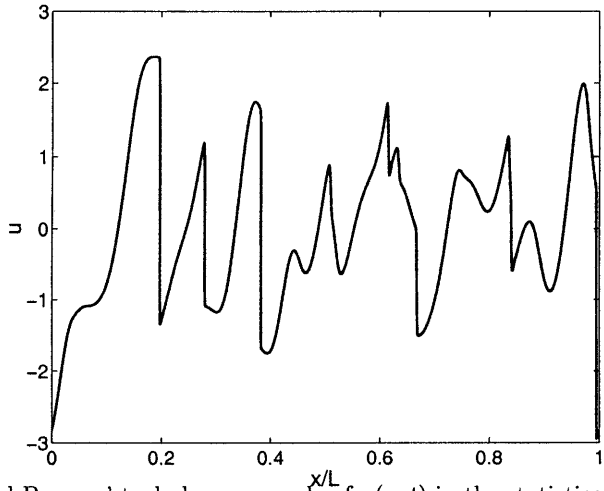

Fig. 8. Forced Burgers' turbulence: sample of $u(x,t)$ in the statistically-stationary state.

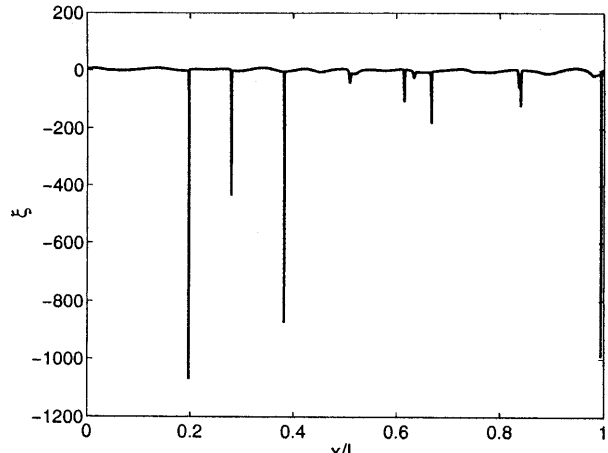

Fig. 9. Sample of $\xi \equiv \partial u/\partial x$ corresponding to Fig. 8.

Figure 10 shows the compensated energy spectra $\kappa^2 E(\kappa)$ obtained from DNS and from LES-PLB with $c_r = 1.0$ and $N = 64$, 256, 1,024 and 4,096. As might be expected, the DNS spectrum exhibits a peak around $\kappa = \kappa_f = 6$. There is then a range ($20 < \kappa < 200$, say) over which the compensated spectrum is approximately constant. This corresponds to the κ^{-2} spectrum that arises because of the shocks. The shocks, however, are in fact smooth; so the spectrum tails off at wavenumbers larger than $\kappa_0 \mathrm{Re}$.

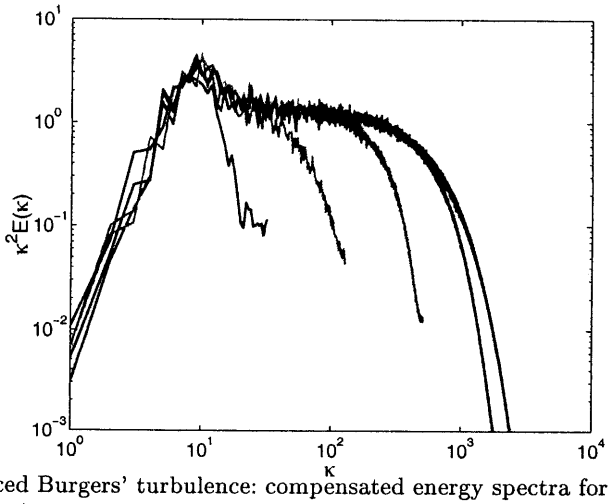

Fig. 10. Forced Burgers' turbulence: compensated energy spectra for (from left to right at large κ): LES-PLB with $c_r = 1.0$, $N = 64$, 256, 1,024 and 4,096; and DNS.

It may be seen from Fig. 10 that LES-PLB behaves in the desired manner. The part of the spectrum that can be well resolved by the given number of ba-

sis functions, N, agrees well with the DNS; whereas the energy is attenuated (by an order of magnitude) at the highest resolved wavenumber.

As may be seen in Fig. 11, the attenuation at the highest wavenumbers depends on the specification of c_r. Lower values result in less attenuation, and in the DNS spectrum being reproduced to higher wavenumbers.

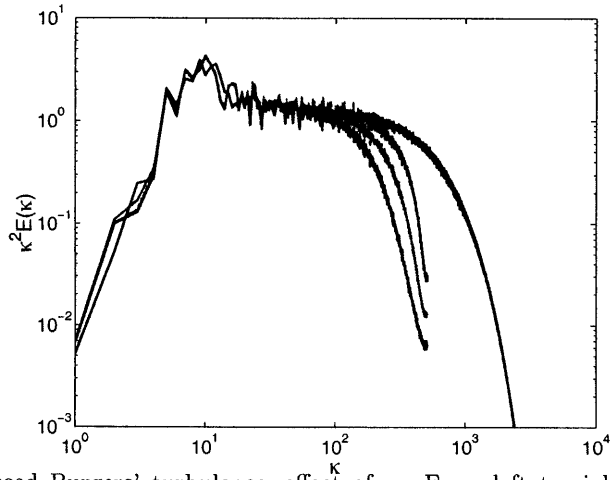

Fig. 11. Forced Burgers' turbulence: effect of c_r. From left to right at large κ, LES-PLB with $N = 1,024$, $c_r = 2.0$, 1.0 and 0.5, and DNS.

Of particular interest in Burgers' turbulence is the PDF of $\xi \equiv \partial u/\partial x$ for negative values of ξ (Gotoh 1999), for this reveals some details of the shocks. Figure 12 shows a log-log plot of the PDF of the normalized gradient ξ/ξ_f for negative ξ. It may be seen that the current DNS results agree well with those of Gotoh. In LES-PLB, since the jump across a shock is of order unity, the steepest gradient that can be represented scales as $1/N$. From Fig. 12 for the case $N = 1,024$, it may be seen that the PDF drops rapidly to zero for $|\xi|/\xi_f$ being larger than 70. The steep gradients that cannot be resolved are smoothed, leading to the increased PDF (compared to DNS) in the range $7 < |\xi|/\xi_f < 70$. While for $|\xi|/\xi_f < 7$, the LES-PLB is in excellent agreement with the DNS.

As in the test case described in the previous section, we find that (for a particular choice of ℓ_s) accurate solutions for the Smagorinsky model produce results comparable to LES-PLB. Figure 13 compares the compensated spectra obtained from LES-PLB ($N = 1,024$, $c_r = 1.0$), with those obtained from the Smagorinsky model (with fixed ℓ_s) with poor ($N = 1,024$) and adequate ($N = 2,048$) numerical resolution. The point is that, using the same number of basis functions as LES-PLB (i.e., $N = 1,024$), the Smagorinsky model solution contains significant numerical errors. More basis functions are needed to implement the Smagorinsky model accurately.

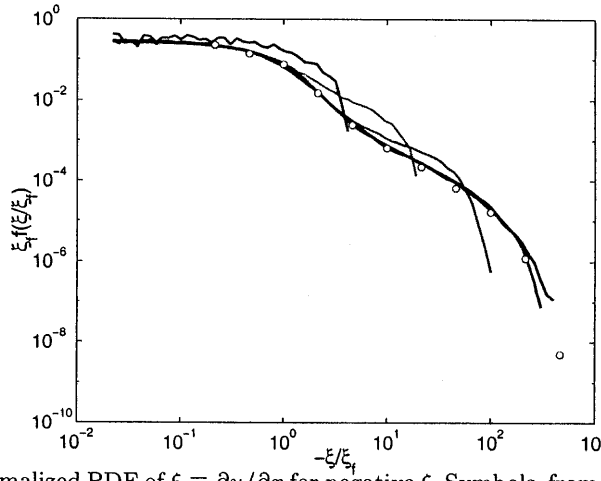

Fig. 12. Normalized PDF of $\xi \equiv \partial u/\partial x$ for negative ξ. Symbols, from Gotoh (1999); lines (from left to right) LES-PLB with $c_r = 1.0$ and $N = 64$, 256, 1,024, 4,096, and DNS.

It may be noted that in most implementations of the dynamic Smagorinsky model (Germano et al. 1991), the Smagorinsky coefficient is taken to be uniform in directions of statistical homogeneity. Hence for the present statistically stationary and homogeneous case, the dynamic model would yield a constant and uniform value of C_s, as used here.

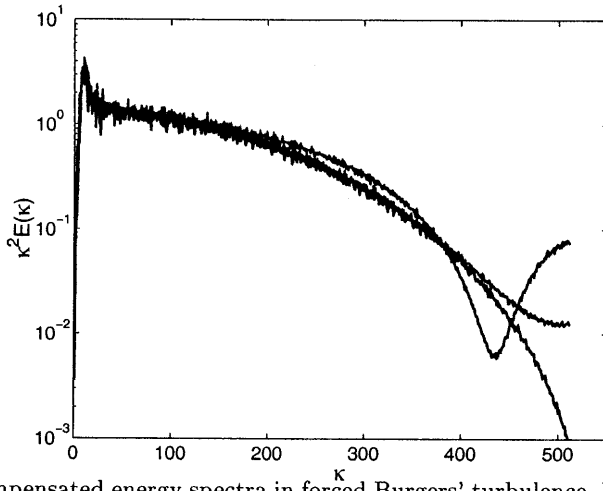

Fig. 13. Compensated energy spectra in forced Burgers' turbulence. From smallest to largest values at high wavenumber: Smagorinsky, $N = 2,048$; LES-PLB, $N = 1,024$; Smagorinsky, $N = 1,024$.

6 Conclusion

A new approach to LES has been developed based on the resolved fields being obtained by projection onto local basis functions. The resulting LES equations are ordinary differential equations for the evolution of the basis-function coefficients. Consequently, in contrast to the traditional filtering approach, there are no issues of numerical spatial discretization and of the consequent numerical errors.

A general model is developed for the effects of the residual motions. This is based directly on the basis-function coefficients, and shares some of the MILES philosophy. The effect of the model is significant only where the rate of change of the field is not well resolved by the basis functions; and its effect is to smooth the field. For linear-spline basis functions, the model resembles an eddy viscosity formulation; whereas with parabolic-spline basis functions it resembles fourth-order dissipation. Needless to say, the LES-PLB methodology would need to be applied to standard turbulent flow test cases (e.g., channel flow) before more general conclusions could be drawn about the efficacy of the modelling of the residual motions.

In the limiting case that the basis functions are sufficient to resolve the instantaneous fields, the LES-PLB methodology reduces to a direct numerical simulation (DNS) using the Galerkin method.

While the LES-PLB methodology is intended for inhomogeneous flows governed by the Navier-Stokes equations, it is demonstrated here for the simpler case of Burgers' equation. The performance of the model is found to be satisfactory in all respects. In contrast, traditional LES computations using the same basis functions exhibit significant numerical error; or, equivalently, significantly more basis functions are required to obtain numerically-accurate solutions.

This initial study leaves many inportant questions still to be answered. How does the method perform with other basis functions, such as cubic splines, or finite-elements? How well does it perform for complex flows governed by the Navier-Stokes equations? And for such flows, what is the computation cost, compared to conventional LES using unstructured grids?

Acknowledgements

It is a pleasure to dedicate this paper to Sid Leibovich on the occasion of his sixtieth birthday. I am grateful to Peter Huang for assistance in performing some of the computations. This work was supported by Air Force Office of Scientific Research Grant No. F49620-97-7-0126.

A Linear-Spline Galerkin Method

In this Appendix, the LES-PLB methodology is explicitly evaluated for Burgers' equation (without forcing), using a sufficient number of linear-spline basis

functions that the residual field is negligible. This corresponds to DNS by a Galerkin method.

In the interval $0 \leq x \leq \mathcal{L}$ there are $N+1$ linear-spline basis functions $b_j(x)$, $j = 0, 1, ..., N$. The jth knot is located at $x_j = jh$, where h is the uniform knot spacing $h = \mathcal{L}/N$. The jth basis function is

$$\begin{aligned} b_j(x) &= 1 - |x - x_j|/h, \quad \text{for} \quad |x - x_j| \leq h, \\ &= 0, \quad \text{for} \quad |x - x_j| \geq h. \end{aligned} \tag{46}$$

The resolved velocity field is

$$\overline{u}(x,t) = \sum_{j=0}^{N} \hat{u}_j(t) b_j(x), \tag{47}$$

where, because of the imposed periodicity, we have $\hat{u}_0(t) = \hat{u}_N(t)$. For the DNS being considered, $\overline{u}$ evolves by Burgers' equation (without forcing):

$$\frac{\partial \overline{u}}{\partial t} = -\overline{u}\frac{\partial \overline{u}}{\partial x} + \nu \frac{\partial^2 \overline{u}}{\partial x^2}. \tag{48}$$

The Galerkin method is obtained from Eq. (48) by substituting Eq. (47) for $\overline{u}$, multiplying by $b_k(x)$ and integrating. The result is

$$M_{jk}\frac{\mathrm{d}\hat{u}_j}{\mathrm{d}t} = -C_{ijk}\hat{u}_i\hat{u}_j + \nu D_{jk}\hat{u}_j, \tag{49}$$

where M_{jk} is given by Eq. (8), C_{ijk} is

$$C_{ijk} \equiv \int_0^{\mathcal{L}} b_i(x) b_j'(x) b_k(x)\, \mathrm{d}x, \tag{50}$$

and D_{jk} is

$$D_{jk} = -\int_0^{\mathcal{L}} b_j'(x) b_k'(x)\, \mathrm{d}x. \tag{51}$$

There is summation over repeated suffixes, and b_j' is written for $\mathrm{d}b_j(x)/\mathrm{d}x$.

Equation (49) and the definition of the coefficients apply to any basis function. For linear splines, the non-zero coefficients are:

$$M_{(j)(j)} = \tfrac{2}{3}h, \quad M_{(j)(j\pm1)} = \tfrac{1}{6}h, \tag{52}$$

$$C_{(j)(j\pm1)(j)} = \pm\tfrac{1}{3}, \quad C_{(j)(j)(j\pm1)} = \mp\tfrac{1}{6}, \tag{53}$$

$$C_{(j)(j\pm1)(j\pm1)} = \pm\tfrac{1}{6}, \tag{54}$$

$$D_{(j)(j)} = -\frac{2}{h}, \quad D_{(j)(j\pm1)} = \frac{1}{h}, \tag{55}$$

where bracketed suffixes are excluded from the summation convention.

Substituting these coefficients into Eq. (49) and dividing by h we obtain

$$\begin{aligned}\frac{\mathrm{d}}{\mathrm{d}t}\left(\tfrac{1}{6}\hat{u}_{k-1} + \tfrac{2}{3}\hat{u}_k + \tfrac{1}{6}\hat{u}_{k+1}\right) = &-\frac{1}{3}\left[\hat{u}_k \frac{(\hat{u}_{k+1} - \hat{u}_{k-1})}{2h}\right] \\ &-\frac{2}{3}\left[\frac{\frac{1}{2}(\hat{u}_{k+1}^2 - \hat{u}_{k-1}^2)}{2h}\right] \\ &+\frac{\nu}{h^2}(\hat{u}_{k+1} - 2\hat{u}_k + \hat{u}_{k-1}).\end{aligned} \tag{56}$$

It may be observed that the right-hand side is identical to a three-point centered finite-difference scheme for Burgers' equation written as

$$\frac{\partial \overline{u}}{\partial t} = -\frac{1}{3}\overline{u}\frac{\partial \overline{u}}{\partial x} - \frac{2}{3}\frac{\partial}{\partial x}\left(\frac{1}{2}\overline{u}^2\right) + \nu\frac{\partial^2 \overline{u}}{\partial x^2}. \tag{57}$$

B Coefficient Matrix for the General Relaxation Model

In this Appendix, the implications of the two requirements imposed in Section 3.5 are evaluated, and hence constraints on the coefficient matrix ω_{ji} in the general relaxation model (Eq. 34) are determined.

B.1 Evaluation of Requirements

For a field that is everywhere unity ($u(x) = 1$), the basis-function coefficients are

$$\hat{B}_j \equiv M_{jk}^{-1} B_k, \tag{58}$$

where B_k is defined by

$$B_k \equiv \int_0^{\mathcal{L}} b_k(x)\,\mathrm{d}x, \tag{59}$$

see Eqs. (6)–(7). Hence for a field that everywhere has the constant value c, the general model Eq. (34) is

$$R_j = \omega_{ji}\hat{B}_i c. \tag{60}$$

The requirement that R_j vanish for such a field leads to the constraint on the coefficient matrix

$$\omega_{ji}\hat{B}_i = 0. \tag{61}$$

With the constant and uniform density taken to be unity, the momentum of the resolved velocity field is

$$\int_0^{\mathcal{L}} \overline{u}(x)\,\mathrm{d}x = B_j \hat{u}_j. \tag{62}$$

Thus the rate of change of momentum due to the modelled term (Eq. 34) is

$$B_j R_j = B_j \omega_{ji} \hat{u}_i. \tag{63}$$

The requirement that the modelled term conserve global momentum for all velocity fields (i.e., all $\hat{u}_i$) therefore imposes the constraint

$$B_j \omega_{ji} = 0. \tag{64}$$

In summary: the general relaxation model Eq. (34) satisfies the two requirements imposed in Section 3.5 provided that the coefficient matrix ω_{ji} satisfies Eqs. (61) and (64).

B.2 General Coefficient Matrix

It is readily verified that Eq. (64) is satisfied by a coefficient matrix ω_{jk} of the form

$$\omega_{jk} = Y_{jk} - \delta_{jk} B_i Y_{i(k)} / B_{(k)}, \tag{65}$$

where Y_{jk} is any $N \times N$ matrix, and bracketed suffixes are excluded from the summation convention.

By substituting Eq. (65) into Eq. (61), we then determine that the condition required to satisfy Eq. (61) is

$$\omega_{jk} \hat{B}_k = Y_{jk} \hat{B}_k - \frac{B_i}{B_{(j)}} Y_{i(j)} \hat{B}_j = 0, \tag{66}$$

or, equivalently

$$\sum_k Z_{jk} = \sum_i Z_{ij}, \tag{67}$$

where

$$Z_{jk} \equiv B_{(j)} Y_{jk} \hat{B}_{(k)}. \tag{68}$$

And a sufficient condition for the satisfaction of Eq. (67) is that Z_{ij} be symmetric.

Having obtained these sufficient conditions, we now construct the general model as follows. We define

$$\omega_{jk} = -\Omega_{(j)} \hat{M}^{(p)}_{jk}, \tag{69}$$

to be the coefficient matrix given by the simple model (see Eq. 35). Then, the symmetric matrix Z_{jk} is defined by

$$Z_{jk} = \tfrac{1}{2}[B_{(j)} \omega_{jk} \hat{B}_{(k)} + B_{(k)} \omega_{kj} \hat{B}_{(j)}]. \tag{70}$$

The corresponding definition of Y_{jk} then follows from Eq. (68)

$$Y_{jk} = \frac{Z_{jk}}{B_{(j)}\hat{B}_{(k)}} = \frac{1}{2}\left[\omega_{jk} + \frac{B_{(k)}\hat{B}_{(j)}}{B_{(j)}\hat{B}_{(k)}}\omega_{kj}\right], \tag{71}$$

and finally ω_{jk} is given by Eq. (65).

B.3 Uniform Basis Functions

The preceding equations simplify significantly for the case of splines (of any order) with uniformly-spaced knots (in any number of dimensions). For then the values of B_j and $\hat{B}_j$ are the same for all j, and Eq. (71) simplifies to

$$Y_{jk} = -\tfrac{1}{2}(\Omega_{(j)} + \Omega_{(k)})\hat{M}^{(p)}_{jk}, \tag{72}$$

(since $\hat{M}^{(p)}_{jk}$ is symmetric).

It may also be noted that if further $\Omega_{(j)}$ is the same for all j (which would not happen in practice) then

$$\omega_{jk} = Y_{jk} = -\Omega_{(j)}\hat{M}^{(p)}_{jk}. \tag{73}$$

B.4 Coefficient Matrix for Linear Splines

For the case of 1D linear-spline basis functions with uniform knot spacing h, the above equations simplify yet further. Direct evaluation of ω_{jk} from Eqs. (72), (65) and (27) yields:

$$\omega_{(j)(j)} = -\tfrac{1}{4}[\Omega_{(j-1)} + 2\Omega_{(j)} + \Omega_{(j+1)}], \tag{74}$$

$$\omega_{(j)(j\pm1)} = \tfrac{1}{4}[\Omega_{(j)} + \Omega_{(j\pm1)}]. \tag{75}$$

Substituting these expressions into Eq. (34) yields the expression for the model R_j given in the text, Eq. (36).

References

1. J. P. Boris, F. F. Grinstein, E. S. Oran, and R. L. Kolbe. New insights into large eddy simulation. *Fluid Dyn. Res.*, 10:199–228, 1992.
2. J. M. Burgers. Application of a model system to illustrate some points of the statistical theory of free turbulence. *Proc. Koninklijke Nederlandse Academie van Wetenschappen*, XLIII:2–12, 1940.
3. B. Galperin and S. A. Orszag. *Large eddy simulation of complex engineering and geophysical flows.* Cambridge University Press, Cambridge, 1993.
4. M. Germano, U. Piomelli, P. Moin, and W. H. Cabot. A dynamic subgrid-scale eddy viscosity model. *Phys. Fluids A*, 3:1760–1765, 1991.

5. S. S. Girimaji and Y. Zhou. Spectrum energy transfer in steady Burgers turbulence. *Phys. Lett. A*, 202:279–287, 1995.
6. T. Gotoh. Probability density functions in steady-state Burgers turbulence. *Phys. Fluids*, 11:2143–2148, 1999.
7. T. Gotoh and R. H. Kraichnan. Statistics of decaying Burgers turbulence. *Phys. Fluids A*, 5:445–457, 1993.
8. D. C. Haworth and K. Jansen. Large-eddy simulation on unstructured deforming meshes: toward reciprocating IC engines. *Comput. and Fluids*, page (in press), 2000.
9. P. Holmes, J. L. Lumley, and G. Berkooz. *Turbulence, coherent structures, dynamical systems, and symmetry.* Cambridge University Press, New York, 1996.
10. A. G. Kravchenko, P. Moin, and R. Moser. Zonal embedded grids for numerical simulations of wall-bounded turbulent flows. *J. Comput. Phys.*, 127:412–423, 1996.
11. A. Leonard. Energy cascade in large eddy simulation of turbulent fluid flow. *Adv. Geophys.*, 18A:237–248, 1974.
12. U. Piomelli. High Reynolds number calculations using the dynamic subgrid-scale stress model. *Phys. Fluids A*, 5:1484–1490, 1993.
13. S. B. Pope. *Turbulent Flows.* Cambridge University Press, Cambridge, 2000.
14. W. C. Reynolds. The potential and limitations of direct and large eddy simulations. In J. L. Lumley, editor, *Whither Turbulence? Turbulence at the Crossroads*, volume 357 of *Lecture Notes in Physics*, pages 313–343. Springer-Verlag, Berlin, 1990.
15. W. Rodi, J. H. Ferziger, M. Breuer, and M. Pourquié. Status of large eddy simulation: results of a workshop. *J. Fluids Eng. Trans. ASME*, 119:248–262, 1997.
16. P. G. Saffman. The large-scale structure of homogeneous turbulence. *J. Fluid Mech.*, 27:581–593, 1967.
17. B. Vreman, B. Geurts, and H. Kuerten. Large-eddy simulation of the turbulent mixing layer. *J. Fluid Mech.*, 339:357–390, 1997.